Progress In Electromagnetics Research C, Vol. 124, 69–79, 2022

A Comparative Investigation on Effect of Coupling in Aperture Coupled Microstrip Antennas

Mahendra P. Yadav, Rajesh K. Singh, and Kamla P. Ray*

Abstract—This paper investigates the electromagnetic coupling from various aperture shapes in aperture coupled suspended rectangular microstrip antennas. The proposed study involves various shapes of coupling aperture such as "rectangle", "H", "bowtie", and "hourglass" with a single-layer aperture coupled suspended rectangular microstrip antenna. Among the various shapes, "hourglass" shaped aperture yields maximum coupling leading to maximum bandwidth. For the validation aperture coupled suspended rectangular microstrip antenna with "hourglass-shaped" aperture is fabricated, and measurements were carried out. The measured fractional impedance bandwidth (FBW) with "hourglass" aperture is more than 30% at 1.06 GHz. Measured peak gain and front-to-back (F/B) ratio of aperture coupled suspended microstrip antenna with "hourglass" at 1.06 GHz are 8.5 dBi and greater than 11.2 dB, respectively. The influence on the antenna's performance parameters such as realized gain, impedance bandwidth, and F/B ratio due to metallic mounting surface is also investigated. The simulated and measured performances of the antenna are in agreement. The proposed investigation is very useful for various applications, when broadband antenna is mounted on a metallic body.

1. INTRODUCTION

The use of aperture coupled microstrip feed in microstrip patch antennas is a convenient technique to achieve broad impedance bandwidth [1]. An aperture coupled suspended microstrip antenna avoids the direct electrical connection between the feed and radiating patch, making it symmetrical, which in turn leads to low cross polarization. The microstrip patch is located on the top substrate, while the microstrip feed line is placed on the bottom substrate. A small aperture in the ground plane is carved to allow coupling from the open-circuited microstrip feed line to the radiating patch. The size, position, and shape of the aperture as well as the tuning length affect the antenna's input impedance. Advantages, such as low cross-pol, low profile, low cost, and conformability, make such antennas appealing [2].

The coupling through "rectangular" and "dogbone" apertures was investigated in [3]. This investigation was with reference to the smallest region of aperture shape that lowers the back radiation; however, numerical results have not been presented. Keeping the aperture length same, coupling through "rectangular", "H", "bowtie" and "hourglass" apertures was investigated [4]. Coupling through H-shaped aperture with various substrates such as air, foam, foam-teflon, and teflon-foam has been investigated [5]. The maximum fractional bandwidth and peak realized gain with an air substrate were reported to be 25% and 8.5 dBi, respectively. Improved radiation characteristics through "H" and "dogbone" with T-shape feed-line were reported [6], but were not validated. Different patch shapes have also been used to study the coupling effect [7]; however, again these data were not validated. The limited fractional bandwidths of 16%, 12%, 2%, and 4% for the rectangular aperture have been reported in [8], [9], [10], and [11], respectively.

Received 30 June 2022, Accepted 25 August 2022, Scheduled 16 September 2022
* Corresponding author: Kamla Prasan Ray (kpray@rediffmail.com).
The authors are with the Electronics Engineering Department, Defence Institute of Advanced Technology, Pune 411025, India.

The coupling through "rectangular", "H-shaped", "dogbone", and "bowtie" apertures was reported in [12], and the realized fractional bandwidths from "rectangular", "dogbone", and "bowtie" apertures were 17%, 20%, and 24%, respectively. However, the paper used two stacked patches which increase the thickness of the antenna. [13] studied the coupling through a "rectangular" aperture without providing any details of the radiation characteristics. [14] investigated the impact of coupling due to changing the position of the patches on top layer with two stacked patches, and the achieved fractional bandwidth was 33%. The fractional bandwidths of 4.5% and 3.8% have been achieved using single patch in [15] by keeping the feed widths 8 mm and 6 mm, respectively.

As discussed above, though researchers have studied coupling from various aperture shapes, a detailed comparative study on various shapes of aperture on the characteristics of a rectangular patch antenna has not been reported. Also, the influence on antenna's performance in the presence of a mounting metallic host plane has not been investigated.

In the proposed work, a detailed study is carried out using different aperture shapes, such as "rectangle", "H", "bowtie", and "hourglass", on the performance of a rectangular patch. It is found that with a single-layer aperture coupled rectangular patch antenna, the maximum electromagnetic coupling has been achieved from an "hourglass" aperture, which yields a fractional impedance bandwidth of more than 30% at 1.06 GHz. The aperture coupled suspended microstrip antenna has been fabricated and tested. The measured and simulated results are in agreement.

Further, the influence on the antenna's performance in terms of realized gain, reflection coefficient, and F/B ratio in the presence of a mounting back plane (metal) of the antenna is also investigated. For obtaining a high gain, impedance bandwidth, and F/B ratio, the minimum distance of the aperture coupled suspended microstrip antenna from the backplane is obtained. The distance between the antenna and backplane can be adjusted to improve the antenna's performance. This result is very useful as most of the applications antenna is mounted on a metallic body.

2. ANTENNA DESIGN

The geometry of an aperture coupled suspended microstrip antenna with a rectangular aperture and a rectangular patch is shown in Fig. 1. All the details of the feed network and the rectangular patch are marked in the figure.

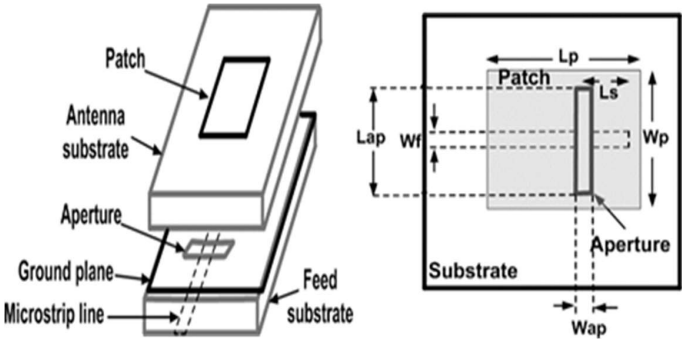

Figure 1. Geometry of an aperture coupled suspended microstrip antenna with rectangular aperture; L_{ap} = length of aperture, W_{ap} = width of aperture, W_f = width of feedline, L_s = length of tuning stub, L_p = length of patch antenna, W_p = width of patch antenna.

The shape of the aperture is an extremely important parameter for achieving maximum coupling in the case of an aperture coupled suspended microstrip antenna. Four different aperture shapes were investigated, which fed the rectangular patch on the top layer. A low-cost FR-4 glass epoxy substrate with relative dielectric constant (ε_r) of 4.3, loss tangent of 0.02, and thickness of 3.2 mm was used to realize the feed of the antenna. The tuning length (L_s) was taken less than $\frac{\lambda_g}{4}$, where λ_g is the wavelength in feed substrate [1]. The length L_s was adjusted in such a way that the maximum coupling is achieved. The optimized value of tuning length (L_s) is 10.66 mm, while the feed line width (W_f)

is 6.2 mm. The optimized thickness of the air substrate is 19 mm for getting maximum impedance bandwidth. The same substrate is used to realize a rectangular microstrip patch antenna except for the thickness of the substrate 1.6 mm. The effective dielectric constant of the antenna is reduced due to the suspended configuration, which, along with aperture coupling, enhances the antenna's impedance bandwidth. In this design, the optimized patch length (L_p) of 100.5 mm and patch width (W_p) of 141 mm were taken for designing the antenna at 1.06 GHz in L-band.

For analyzing the effect of coupling and the performance of the antennas, various apertures shapes such as "rectangle", "H", "bowtie", and "hourglass" were designed [2]. These apertures were used to excite the rectangular patch fabricated on a glass epoxy substrate with an air gap in between the aperture and the substrate [2]. The side view of an aperture coupled microstrip antenna is shown in Fig. 2. The CST Microwave Studio is used to carry out the simulations. Analysis of the circuit can also be done after obtaining the equivalent circuit of an aperture coupled microstrip antenna, as shown in Fig. 3. The input impedance of the full layout of the antenna can be calculated from the knowledge of the equivalent circuit, and reflection coefficient of the circuit can be plotted. The total input impedance (Z_{in}) of an aperture coupled microstrip patch antenna is the combination of impedances Z_{in1} and Z_{in2} as shown in Fig. 3. In the present work, we have studied the impact of different aperture shapes on the antenna performance. It is rather difficult to readily get accurate values of components (R_{ap}, C_{ap}, and L_{ap}) of an equivalent circuit for small variations in the aperture shapes as shown in Fig. 4. Therefore, we have analyzed the aperture coupled suspended rectangular patch antenna for various aperture shapes with the help of full-wave analysis based CST microwave studio. By using this software, accurate analysis of the impact of minute variations in the aperture geometry has been obtained.

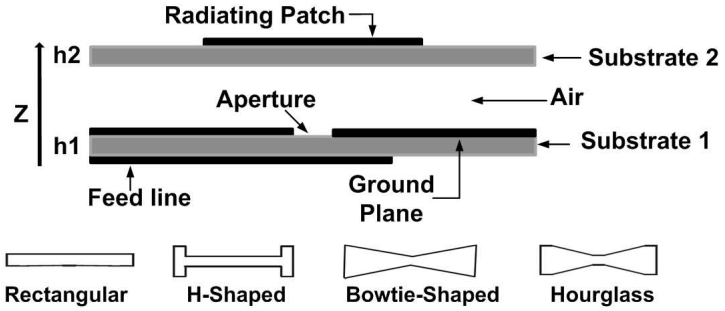

Figure 2. Side view of an aperture coupled microstrip patch antenna.

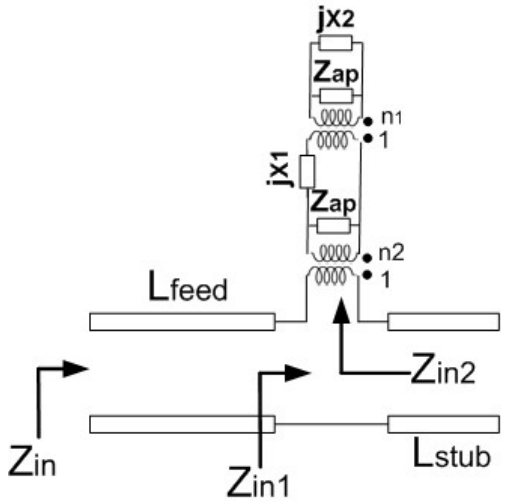

Figure 3. Equivalent circuit of an aperture coupled microstrip patch antenna, (jX_1 and jX_2 are the reactances, L_{feed} is the inductance of the feed line, L_{stub} is the inductance of the stub as shown in Fig. 1).

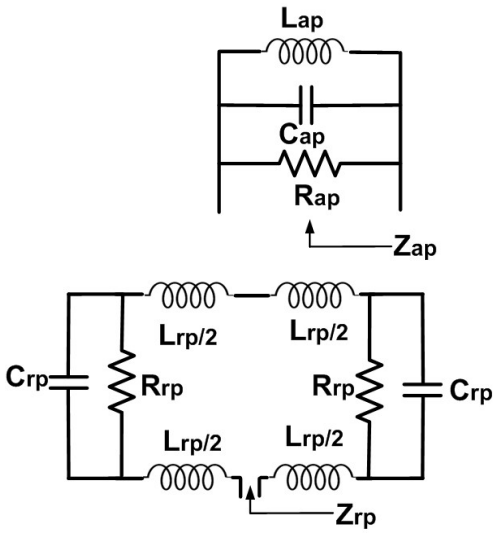

Figure 4. Equivalent circuit for the calculation of impedances, Z_{ap} and Z_{rp} from the equivalent circuit of the aperture and radiating element, respectively (R_{rp}, L_{rp} and C_{rp} are the equivalent resistance, inductance and capacitance, respectively for the radiating patch while Rap, Lap and Cap for the aperture).

3. EFFECT ON INPUT IMPEDANCE OF APERTURE COUPLED SUSPENDED MICROSTRIP ANTENNA USING DIFFERENT APERTURES

3.1. Rectangular Aperture

Figure 5(a) depicts the geometry of a "rectangular" aperture. The non-resonant optimum aperture length ($L_{ap} = AP$) for a rectangular aperture is calculated as 70 mm. Initially, the aperture width ($W_{ap} = AB$) is chosen to be the same as the width of the feedline (W_f) of 6.2 mm, which is non-resonant. The coupling was further increased by varying the aperture width (AB) by keeping the length AP fixed. As illustrated in Fig. 5(b), when AB increases from 6.2 to 7.6 mm, the loop size within Voltage Standing Wave Ratio (VSWR) = 2 circle increases, indicating the increase in the coupling. This facilitates the increase in larger frequency component within VSWR = 2 circle leading to increase in the impedance bandwidth. When AB decreases from 6.2 to 5.2 mm, the loop size decreases. The optimized fractional

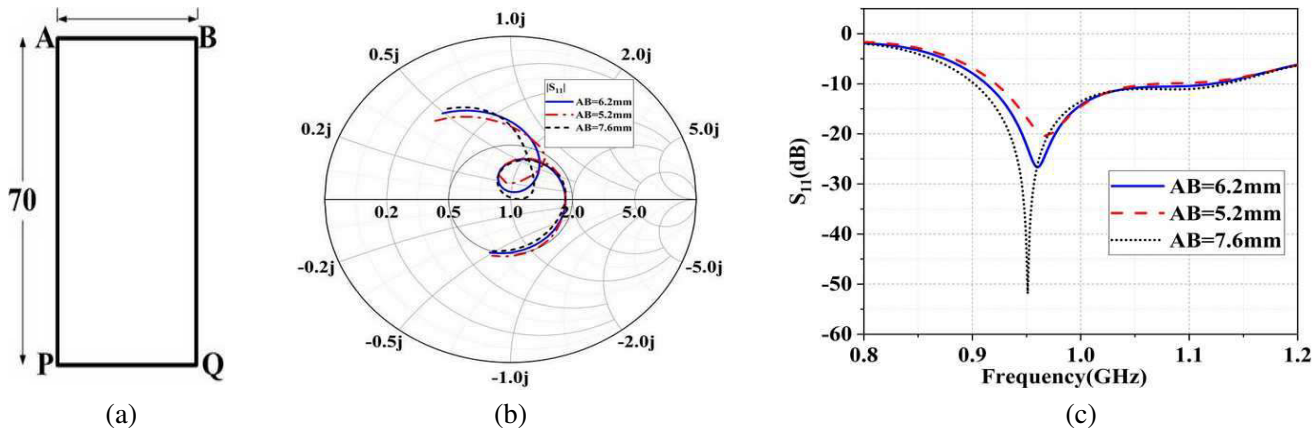

(a) (b) (c)

Figure 5. (a) Geometry of rectangular aperture ($AP = L_{ap} = 70$ mm, $AB = PQ$). (b) Simulated input impedance loci showing the effects of variation of the width AB of the "rectangular" aperture. (c) Reflection coefficients of "rectangular" aperture for different widths AB.

Table 1. Result summary for "rectangular" aperture.

AP (mm)	AB (mm)	Impedance Bandwidth (GHz)	(%) FBW
70	6.2	0.910–1.122	20.9
70	5.2	0.921–1.067	14.7
70	7.6	0.903–1.130	22.3

impedance bandwidth is 22.3% for $AB = 7.6$ mm. Reflection coefficient plot showing the impedance bandwidth is plotted in Fig. 5(c). The overall results are summarized in Table 1.

3.2. H-Shaped Aperture

Figure 6(a) depicts the geometry of an "H' shaped aperture. The overall length AP of the aperture is kept fixed at 70 mm, which is the same as the earlier case of rectangular aperture. The center and edge widths OM and AB are varied to examine the coupling effect. Initially, $OM = 5$ mm and $AB = 10$ mm were chosen as a starting point, and the coupling effect was investigated. The parametric analysis was carried out by varying OM from 3 mm to 8 mm while keeping AB constant. Similarly, parametric studies of AB from 8 mm to 14 mm have been performed while keeping OM constant. Fig. 6(b) shows the variation of input impedance loci for variation of aperture widths OM and AB. Likewise, the reflection coefficient plots showing the impedance bandwidth are depicted in Fig. 6(c). It is noted that loop sizes of impedance loci within VSWR = 2 circle are bigger, indicating higher coupling for the H-shaped aperture. Results summery is given in Table 2. For $OM = 6.2$ mm and $AB = 12.4$ mm, a bigger loop size of impedance loci within the VSWR = 2 circle yields a bandwidth of 28.3%.

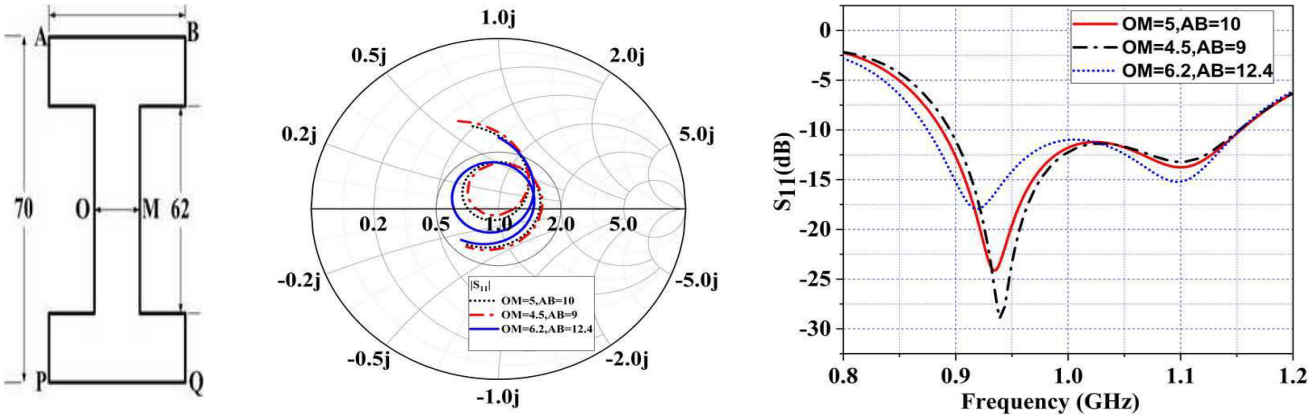

(a) (b) (c)

Figure 6. (a) Geometry of "H" shaped aperture ($AP = L_{ap} = 70$ mm, OM = center width, $AB = PQ$ = edge width). (b) Simulated input impedance loci showing the effects of variations of the OM and AB of "H-shaped" aperture. (c) Reflection coefficients of "H-shaped" aperture at different widths (OM and AB).

Table 2. Results summary for "H-shaped" aperture.

AP (mm)	OM (mm)	AB (mm)	Impedance bandwidth (GHz)	(%) FBW
70	4.5	9	0.895–1.151	25.0
70	5	10	0.887–1.154	26.1
70	6.2	12.4	0.867–1.153	28.3

3.3. Bowtie-Shaped Aperture

For the analysis, the overall aperture length AP of the "bowtie" aperture, which is shown in Fig. 7(a), is fixed at 70 mm, which is the same as those of two apertures discussed earlier. To study the coupling effect, the center width OM and edge width AB of the bowtie are varied. As discussed in earlier cases, the parametric analysis of OM and AB has been investigated. Fig. 7(b) shows the variation of input impedance loci for variation of aperture widths. The corresponding reflection coefficient plots showing the impedance bandwidth are plotted in Fig. 7(c).

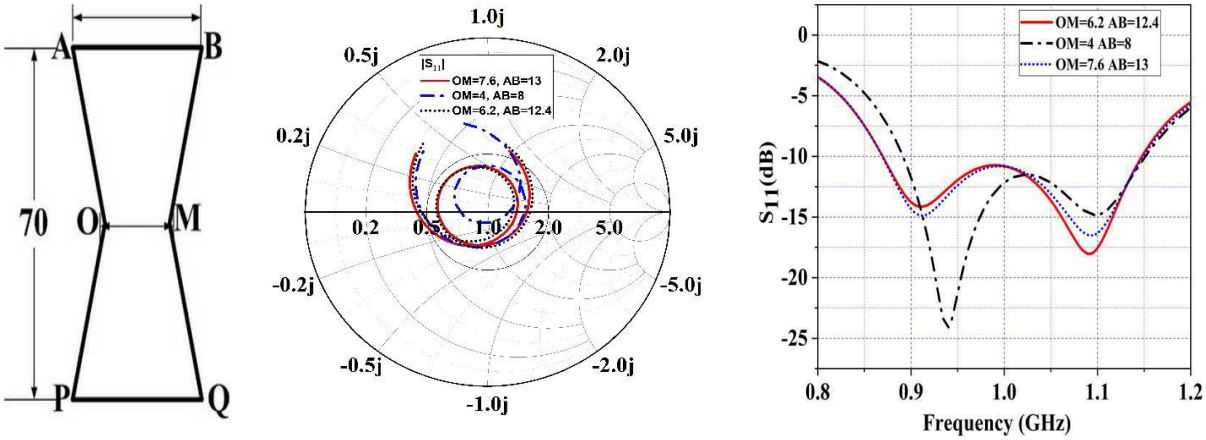

(a) (b) (c)

Figure 7. (a) Geometry of "bowtie" aperture ($AP = L_{ap} = 70$ mm, OM = center width, $AB = PQ$ = edge width). (b) Simulated input impedance loci showing the effect of variations of the OM and AB of the "bowtie" aperture. (c) Reflection coefficients of "bowtie" aperture at different widths (OM and AB).

In the case of bowtie aperture, the loop size of the impedance loci within VSWR = 2 circle is also bigger than that of the rectangular aperture, indicating increased coupling to the patch. Table 3 summarizes results for three values of OM and AB. For $OM = 7.6$ mm and $AB = 13$ mm, the loop size within the VSWR = 2 circle is the biggest, which in turn yields the bandwidth of 27.7% at 1.06 GHz.

Table 3. Results summary for "bowtie" aperture.

AP (mm)	OM (mm)	AB (mm)	Impedance bandwidth (GHz)	(%) FBW
70	6.2	12.4	0.869–1.147	27.6
70	4	8	0.891–1.151	25.4
70	7.6	13	0.869–1.148	27.7

3.4. Hourglass-Shaped Aperture

Finally, Fig. 8(a) depicts the geometry of an"hourglass" aperture, which illuminates the rectangular patch. For this aperture also, the length of the aperture for comparative study is kept the same as $AP = 70$ mm, while the center width OM and edge width AB are varied. The parametric analysis of OM was carried out for 4 mm to 8 mm, while keeping AB constant. Similarly, parametric study of AB was performed for variation from 9 mm to 14 mm keeping OM constant. Fig. 8(b) shows the variation of input impedance loci with aperture width. The optimized loop sizes for "H", "bowtie", and "hourglass" are similar. However, the larger loop within the VSWR = 2 circle is yielded by an "hourglass" aperture. The reflection coefficient plots showing the impedance bandwidth are shown in Fig. 8(c), and results are summarized in Table 4.

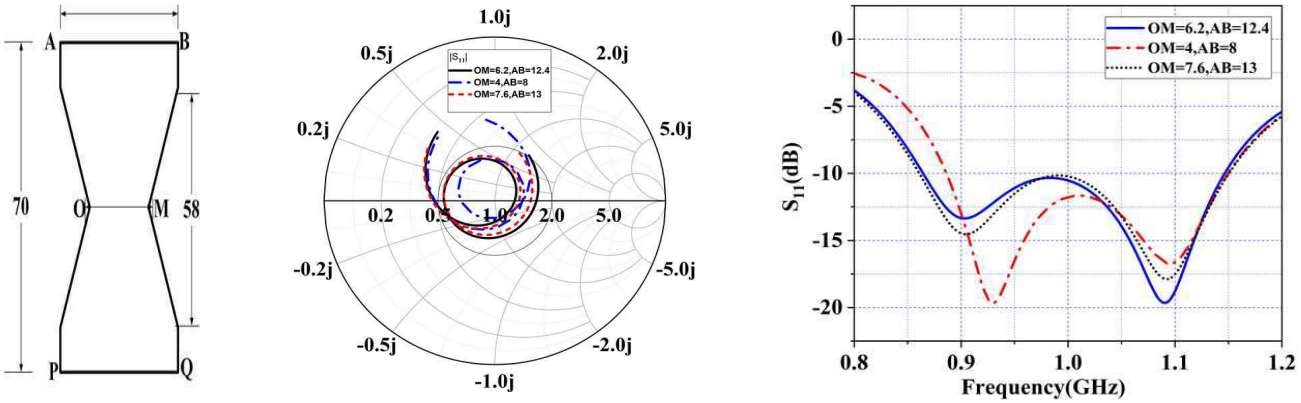

(a) (b) (c)

Figure 8. (a) Geometry of "hourglass" aperture ($AP = L_{ap} = 70\,\text{mm}$, OM = center width, $AB = PQ$ = edge width). (b) Simulated input impedance loci showing the effect of variations of the width OM and AB of the "hourglass" aperture for fixed $AP = L_{ap} = 70\,\text{mm}$. (c) Reflection coefficients of "hourglass" aperture at different widths (OM and AB and $AP = L_{ap} = 70\,\text{mm}$).

Table 4. Results summary for "hourglass" aperture.

AP (mm)	OM (mm)	AB (mm)	Impedance bandwidth (GHz)	(%) FBW
70	6.2	12.4	0.864–1.146	28.0
70	4	8	0.886–1.149	25.8
70	7.6	13	0.861–1.150	28.7

The simulated optimized impedance bandwidths of the "rectangular", "H-shaped", "bowtie", and "hourglass" apertures are 22.3%, 28.3%, 27.7%, and 28.7%, respectively. The maximum coupling and impedance bandwidth are obtained through the "hourglass" aperture. Therefore, for experimental validation, it was fabricated, and measurements were carried out on this configuration. Fig. 9 shows the fabricated antenna with "hourglass" aperture.

(a) (b) (c)

Figure 9. Photographs of fabricated aperture coupled suspended microstrip antenna; (a) hourglass aperture, (b) feed line, (c) integrated aperture coupled suspended microstrip antenna with rectangular patch.

Aperture coupled suspended microstrip antenna with "hourglass" aperture is fabricated on a low cost FR4 substrate. Relatively higher loss tangent of 0.02 does not affect the performance of the antenna at lower frequency of L-band. Further, there is air gap in between making it suspended, which reduces the overall loss tangent. A handheld vector network analyzer (model: N9916A) is used to test the fabricated antenna. Simulated and measured reflection coefficient plots are compared in Fig. 10. It shows a good agreement between the measured and simulated impedance bandwidths, which are from 0.855 GHz to 1.161 GHz (30%) and from 0.861 GHz to 1.150 GHz (28.8%), respectively.

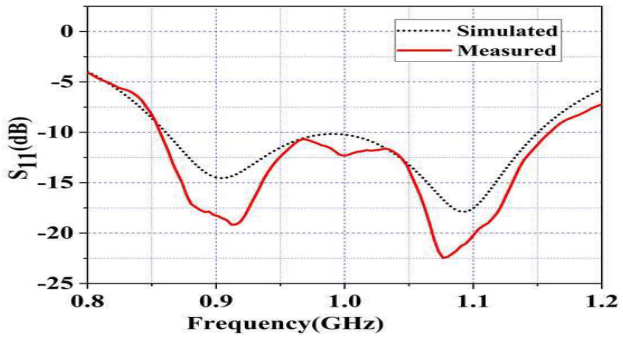

Figure 10. Simulated and measured reflection coefficient of aperture coupled suspended microstrip antenna with "hourglass" aperture.

4. APERTURE COUPLED SUSPENDED MICROSTRIP ANTENNA WITH METAL BACKPLANE

These apertures coupled suspended microstrip antennas are commonly mounted on a metallic host surface. The performance of the antenna may change after placing it on a metallic body. Thus, the effect of the metallic host body on the performance of the aperture coupled suspended microstrip antenna needs to be investigated, which is not reported so far. An aperture coupled suspended rectangular microstrip antenna, fed by an "hourglass" aperture, which yielded maximum bandwidth, is considered for further investigation. Metallic backplane is placed just below the antenna (feed side), and simulations were carried out by varying the gap between feed line of the aperture coupled suspended microstrip antenna and mounting metallic ground plane. It was observed that the performances such as impedance bandwidth, gain, and F/B ratio are affected in the presence of mounting ground plane. The performance

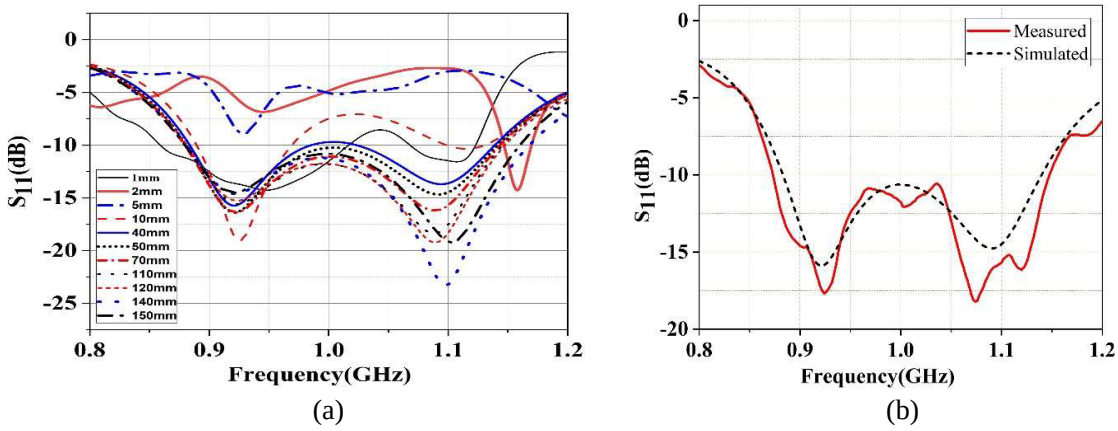

Figure 11. (a) Simulated reflection coefficients for different gaps between the antenna and backplane. (b) Simulated and measured reflection coefficient with backplane at 50 mm of aperture coupled suspended microstrip antennas with "hourglass" aperture.

of the antenna depends on the gap between the antenna and backplane, as the back radiation from the aperture in the ground plane gets affected. Fig. 11(a) depicts the simulated impedance bandwidth at different gaps, and the corresponding gain and F/B ratio at different gaps are summarized in Table 5. For the 50 mm gap between the antenna and backplane, the gain is 8.18 dBi, and the F/B ratio is 25.1 dB with measured and simulated bandwidths similar to that of the optimized aperture coupled antenna with an"hourglass" aperture as shown in Fig. 11(b).

Table 5. Results summary by varying the gap between the antenna and metallic backplane.

Distance (mm)	1	2	5	10	40	50	70	110	120	140	150
Gain (dBi)	3.77	3.19	4.50	6.77	7.70	8.18	9.13	10.10	10.20	9.78	7.88
F/B ratio (dB)	24.4	26.1	28.8	28.5	28.5	25.1	25.2	24	23.20	19.7	15.2

5. RADIATION PATTERN

The radiation pattern of this antenna was measured in an anechoic chamber as shown in Fig. 12(a). The photograph shows the measurement setup, wherein the receiving antenna is mounted on a turn table, which rotates horizontally. On the other end, a transmitting antenna is mounted. The distance between antennas is taken after satisfying the far-field criterion. Received power is measured by means of a handheld spectrum analyzer (N9916A). A Rohde & Schwarz vector signal generator (SMU200A, 100 kHz–6 GHz) is used to feed RF power to transmitting antenna. The measured and simulated normalized radiation patterns of the proposed antenna with an "hourglass" aperture at 1.06 GHz are shown in Figs. 12(b)–(e).

Table 6. Comparison of bandwidth of different aperture shapes in aperture coupled suspended microstrip antenna.

Ref	Types of Aperture shapes	Freq. Range (GHz)	Center frequency (GHz)	% Bandwidth	Geometry type/layer
[3]	Rectangular Dogbone	-	3.5	-	Single patch
[8]	Rectangular	4.5–5.25	-	16	Single patch*
[9]	Rectangular	-	1.25	12	Single patch
[10]	Rectangular	-	-	2	Single patch
[11]	Rectangular	0.9–1.07	-	17	Stacked patches*
	Dogbone	0.90–1.1	-	20	
	Bowtie	0.88–1.12	-	24	
[14]	Rectangular	9.5–16	-	33	Stacked patches*
Present work	**Rectangular**	**0.903–1.130**	**≈ 1.06**	**22.3**	**Rectangular Single Patch**
	H-shaped	**0.867–1.153**		**28.3**	
	Bowtie	**0.869–1.148**		**27.7**	
	Hourglass	**0.861–1.150**		**30.0 (measured)**	

*Estimated from the data given in the paper

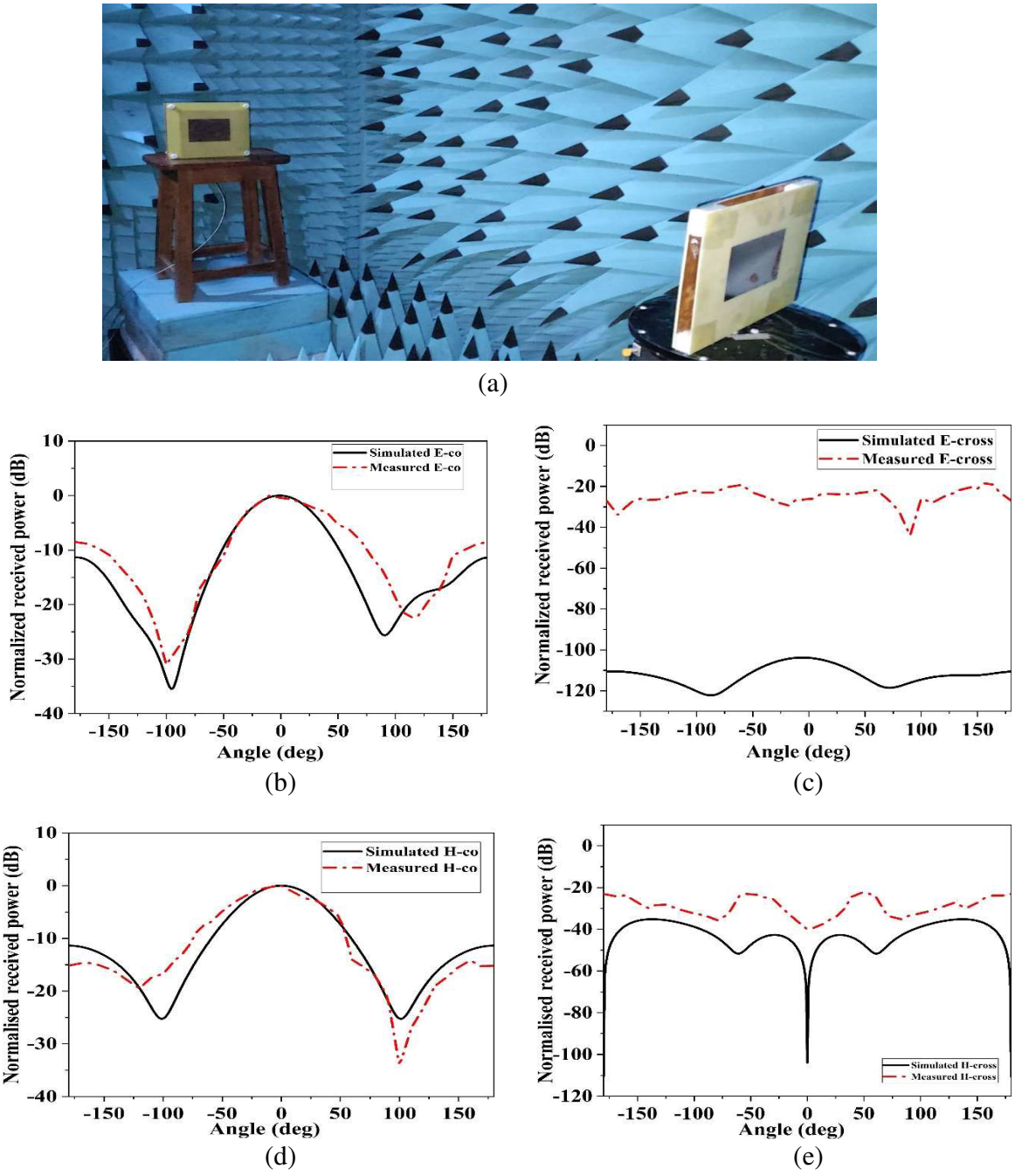

Figure 12. Simulated and measured normalized radiation patterns of antenna with "hourglass" aperture at 1.06 GHz. (a) Measurement setup, (b) E-co, (c) E-cross, (d) H-co and (e) H-cross.

At 1.06 GHz, the measured F/B ratio and gain of antenna are greater than 11.2 and 8.5 dBi, respectively. The measured 3 dB beamwidth is 55° in E plane, whereas it is 62.4° in H-plane. To clearly bring out the findings of the investigation on coupling of various aperture shapes to the suspended rectangular patch on a glass epoxy substrate, a comparison of various reported configurations with different aperture shapes is summarized in Table 6. It is noted that an "hourglass" aperture gives maximum coupling to the single suspended rectangular patch leading to improved measured bandwidth of 30% at 1.06 GHz.

6. CONCLUSIONS

Four different apertures, namely "rectangle", "H", "bowtie", and "hourglass" were investigated for the coupling of a suspended rectangular patch on a glass epoxy substrate. A single-layer suspended rectangular patch antenna with "hourglass" aperture yielded maximum coupling and hence the impedance bandwidth. The measured fractional impedance bandwidth was greater than 30% at center frequency of 1.06 GHz with "hourglass" aperture which agrees well with the simulated data. The influence on the antenna's performance parameters such as realized gain, impedance BW, and F/B ratio because of the metallic host ground plane was also investigated. The proposed investigation is useful as these antennas are commonly mounted on a metallic host structure. This antenna is developed for the L-band Identification Friend or Foe (IFF) system.

REFERENCES

1. Pozar, D. M., "A review of aperture coupled microstrip antennas: History, operation, development, and applications," 1–9, University of Massachusetts at Amherst, 1996.
2. Kumar, G. and K. P. Ray, *Broadband Microstrip Antennas*, Artech House, 2003.
3. Pozar, D. M. and S. D. Targonski, "Improved coupling for aperture coupled microstrip antennas," *Electronics Letters*, Vol. 27, No. 13, 1129–1131, 1991.
4. Rathi, V., G. Kumar, and K. P. Ray, "Improved coupling for aperture coupled microstrip antennas," *IEEE Transactions on Antennas and Propagation*, Vol. 44, No. 8, 1196–1198, 1996.
5. Jazi, M. N., Z. H. Firouzeh, H. Mirmohammad-Sadeghi, and G. Askari, "Design and implementation of aperture coupled microstrip IFF antenna," *PIERS Proceedings*, 198–202, Hangzhou, China, March 24–28, 2008.
6. Aijaz, Z. and S. C. Shrivastava, "An introduction of aperture coupled microstrip slot antenna," *International Journal of Engineering Science and Technology*, Vol. 2, No. 1, 36–39, 2010.
7. Aijaz, Z. and S. C. Shrivastava, "Effect of the different shapes: Aperture coupled microstrip slot antenna," *International Journal of Electronics Engineering*, Vol. 2, No. 1, 103–105, 2010.
8. Aijaz, Z. and S. C. Shrivastava, "Coupling effects of aperture coupled microstrip antenna," *International Journal of Engineering Trends and Technology*, Vol. 20, No. 11, 2011.
9. Rathod, J. M., "Comparative study of microstrip patch antenna for wireless communication application," *International Journal of Innovation, Management and Technology*, Vol. 1, No. 2, 194–197, 2010.
10. Singh, M., A. Basu, and S. K. Koul, "Design of aperture coupled fed micro-strip patch antenna for wireless communication," *2006 Annual IEEE India Conference*, IEEE, 2006.
11. Kharade, S. A., S. V. Khobragade, and A. Bagwari, "An aperture coupled microstrip patch antenna for application at 7.5 GHz," *International Journal of Engineering Research & Technology (IJERT)*, Vol. 8, No. 7, July 2019.
12. Jiang, H. and K. Cho, "Novel broadband aperture-coupled patch antenna using bow-tie shaped slot," *Proc. ISAP 2006, Session D*, 2006.
13. Anandkumar, D. and R. G. Sangeetha, "Design and analysis of aperture coupled micro strip patch antenna for radar applications," *International Journal of Intelligent Networks*, Vol. 1, 141–147, 2020.
14. Ghassemi, N., J. Rashed-Mohassel, M. H. Neshati, S. Tavakoli, and M. Ghassemi, "A high gain dual stacked aperture coupled microstrip antenna for wideband applications," *Progress In Electromagnetics Research B*, Vol. 9, 127–135, 2008.
15. Rahim, M. K. A., et al., "Aperture coupled microstrip antenna with different feed sizes and aperture positions," *2006 International RF and Microwave Conference*, IEEE, 2006.